Research Article

Modular Extracellular Sensor Architecture for Engineering Mammalian Cell-based Devices

Nichole M. Daringer,[†] Rachel M. Dudek,[†] Kelly A. Schwarz,[†] and Joshua N. Leonard[†,‡,§,*]

[†]Department of Chemical and Biological Engineering, Northwestern University, Evanston, Illinois 60208, United States
[‡]Chemistry of Life Processes Institute, Northwestern University, Evanston, Illinois 60208, United States
[§]Member, Robert H. Lurie Comprehensive Cancer Center, Northwestern University, Evanston, Illinois 60208, United States

Ⓢ Supporting Information

ABSTRACT: Engineering mammalian cell-based devices that monitor and therapeutically modulate human physiology is a promising and emerging frontier in clinical synthetic biology. However, realizing this vision will require new technologies enabling engineered circuitry to sense and respond to physiologically relevant cues. No existing technology enables an engineered cell to sense exclusively extracellular ligands, including proteins and pathogens, without relying upon native cellular receptors or signal transduction pathways that may be subject to crosstalk with native cellular components. To address this need, we here report a technology we term a Modular Extracellular Sensor Architecture (MESA). This self-contained receptor and signal transduction platform is maximally orthogonal to native cellular processes and comprises independent, tunable protein modules that enable performance optimization and straightforward engineering of novel MESA that recognize novel ligands. We demonstrate ligand-inducible activation of MESA signaling, optimization of receptor performance using design-based approaches, and generation of MESA biosensors that produce outputs in the form of either transcriptional regulation or transcription-independent reconstitution of enzymatic activity. This systematic, quantitative platform characterization provides a framework for engineering MESA to recognize novel ligands and for integrating these sensors into diverse mammalian synthetic biology applications.

KEYWORDS: mammalian synthetic biology, receptor engineering, biosensor, cell therapy
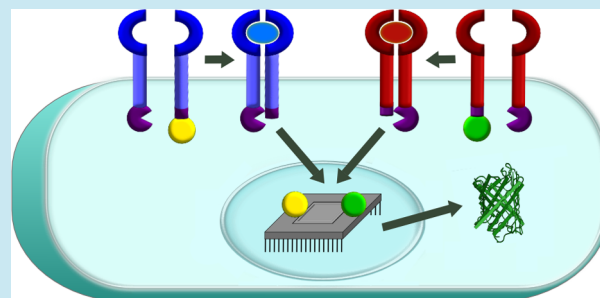
The ability to engineer mammalian cellular devices that sense and respond to their environment in defined ways would enable the construction of sophisticated cell-based therapeutics and transformative tools for fundamental biological research. Such capabilities could overcome persistent barriers to treatment in applications ranging from cancer immunotherapy to regenerative medicine. Synthetic biology provides such an approach for building novel cellular functions from the bottom up, and the toolbox of biological parts that operate in mammalian cells is rapidly expanding. In particular, nucleic acid and protein-based sensors have been developed to recognize diverse ligands including small biomolecules such as vitamins[1,2] and metabolites,[3] chemical species such as acetaldehydes and nitric oxide,[4,5] environmental conditions such as hypoxia,[6,7] and even defined combinations of small molecules[8] or RNA.[9] Notably, each of these sensing events occurs in the cytoplasm of the engineered cell, such that these approaches do not enable cell-based devices to sense many species of biological relevance, including cytokines, chemokines, cell-surface antigens, and pathogens, which are exclusively extracellular. Therefore, engineering cell-based devices that interface robustly with host physiology necessitates new technologies for engineering cell-surface biosensors that transduce the detection of exclusively extracellular ligands into changes in cell state.

One approach to building a biosensor for a given ligand is to modify an existing biosensor protein to recognize a new input. For example, directed evolution of G-protein coupled receptors (GPCRs) has generated receptors with novel specificities (receptors activated by solely synthetic ligands, or RASSLs) for drug-like small molecules.[10,11] In addition, technologies for genetically engineering novel immune receptors, termed chimeric antigen receptors (CAR), enable programming T cells to respond to defined ligands, and this approach has recently demonstrated great promise for cancer immunotherapy in both preclinical[12−14] and clinical investigations.[15−17] A limitation of all these approaches is that these novel receptors utilize native downstream signaling mechanisms to transduce a detection event into a change in cell state. Therefore, signaling downstream from the engineered receptors may be subject to cross-talk or regulation by native cellular pathways and components. Moreover, these sensing events may be transduced into signaling via complex biophysical mechanisms,[18] precluding the straightforward redirection of receptor

output into engineered gene circuits. Thus, integrating such modified receptors into complex synthetic biology "programs" will require new engineering strategies.[19]

An alternative approach for coupling ligand-binding to changes in cell state is to redirect native receptor sensing and signaling into orthogonal pathways. Most notably, the Tango assay enables one to detect a ligand binding-induced protein–protein interaction by transducing this association into the release of an engineered transcription factor from an inactive state.[20] In this system, the transcription factor is genetically tethered to a cell surface receptor protein via an amino acid sequence that is cleaved by the Tobacco Etch Virus protease (TEV), and TEV is genetically tethered to an adaptor protein that is recruited to the receptor when the receptor is in the ligand-bound state. Thus, binding of ligand to the receptor brings TEV into proximity with its target sequence, resulting in a trans-cleavage event that liberates the transcription factor to translocate to the nucleus and regulate expression of an engineered reporter gene. Other approaches for monitoring native protein–protein interactions include split protein reconstitution, in which a protein such as GFP[21] or TEV[22] is genetically split, with N- and C terminal domains fused to each of two interaction partners, such that association between the interaction partners enables the split GFP or TEV to refold and reconstitute its activity. While these approaches do redirect ligand binding-induced receptor signaling into orthogonal signaling pathways, they nonetheless rely on native interactions and may interact with native cellular components. Moreover, receptor redirection requires existing native receptors and adapter proteins, potentially limiting the generalizability and portability of this approach. Thus, while several useful tools for biosensing exist, a general approach for engineering biosensors for exclusively extracellular ligands represents an important technology gap in mammalian synthetic biology.

To meet this need, we have developed a technology we term a Modular Extracellular Sensor Architecture (MESA). Here, we describe the design and development of the MESA platform, comprising independent, tunable modules, and the optimization of MESA performance using design-based approaches. We demonstrate ligand-inducible activation of MESA signaling and adaptation of the MESA platform to generate either transcription-dependent or transcription-independent outputs. Through the systematic characterization of this platform, we provide a quantitative framework that should streamline the adaptation of the MESA system to recognize novel ligands and the integration of these sensors into various synthetic biology functional programs.

RESULTS AND DISCUSSION

The MESA design concept (Figure 1) comprises a fully self-contained sensing and signal transduction system, such that binding of ligand to the receptor induces signaling via an orthogonal mechanism to regulate expression of a target gene. In our initial MESA design, ligand binding-induced receptor dimerization results in proteolytic trans-cleavage of the target chain (TC) by the protease chain (PC), releasing a transcription factor (TF) previously sequestered at the plasma membrane. Such a transcription factor might be either a native protein or a protein engineered using zinc-finger[23] or TALE[24] DNA-binding domains to regulate expression of either native or exogenously introduced genes. The ectodomain (ECD) confers both specificity and affinity for a ligand. Potential ectodomain sources include ligand-binding domains from native receptors,
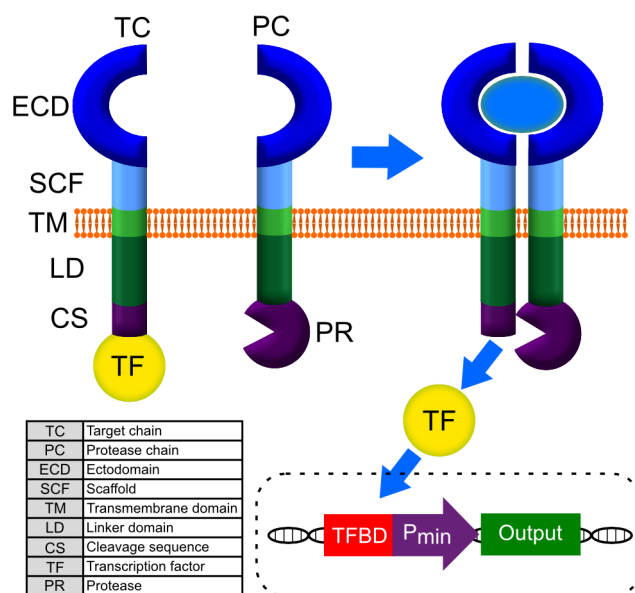

TC	Target chain
PC	Protease chain
ECD	Ectodomain
SCF	Scaffold
TM	Transmembrane domain
LD	Linker domain
CS	Cleavage sequence
TF	Transcription factor
PR	Protease

Figure 1. Modular extracellular sensor architecture (MESA) design concept. Proposed general mechanism: ligand binding-induced receptor dimerization causes the protease on the protease chain (PC) to cleave its cognate cleavage sequence on the target chain (TC), which releases the transcription factor (TF) to travel to the nucleus and modulate target gene expression by binding to a TF binding domain (TFBD) adjacent to a minimal promoter (P_{min}) to drive expression of the output gene.

short chain variable fragments (scFv) derived from monoclonal antibodies, or any other protein(s) that dimerizes upon ligand binding. Ligand binding may be homotypic in the case of multivalent ligands (e.g., many cytokines exist as homodimers), such that the ectodomain on each MESA chain recognizes the same epitope. Ligand binding may also by heterotypic, such that the ectodomain on each MESA chain binds to a distinct epitope on a given ligand. The transmembrane domain (TMD) confers cell surface localization.

A key feature of MESA design is the use of modular domains to enable performance optimization by "tuning" receptor biophysics. Desirable performance characteristics may include low background in the absence of ligand, a high signal-to-noise ratio, and a large or small dynamic range (depending on the application), wherein the magnitude of MESA output depends on analyte concentration. For example, cleavage kinetics may be directly modulated by modifying either the protease (PR) on the PC or the protease's cognate cleavage sequence (CS) on the TC. Receptor geometry and steric interactions may be tuned via both the extracellular scaffold (SCF), located between the ectodomain and transmembrane domain, or the intracellular linker domain (LD), located between the transmembrane domain and cleavage sequence. Each of these experimental handles for protein engineering was systematically explored to map out MESA design space.

Characterization of MESA Design Space Using Model Receptors. To initially evaluate the feasibility of the MESA concept, we developed a strategy enabling us to decouple the two engineering goals required to build a functional MESA: (1) achieve ligand binding-induced receptor dimerization and (2) achieve receptor dimerization-induced signaling. To pursue the latter goal first and identify intracellular receptor architectures that confer dimerization-inducible signaling, a small library of model receptors was constructed in which receptor dimeriza-
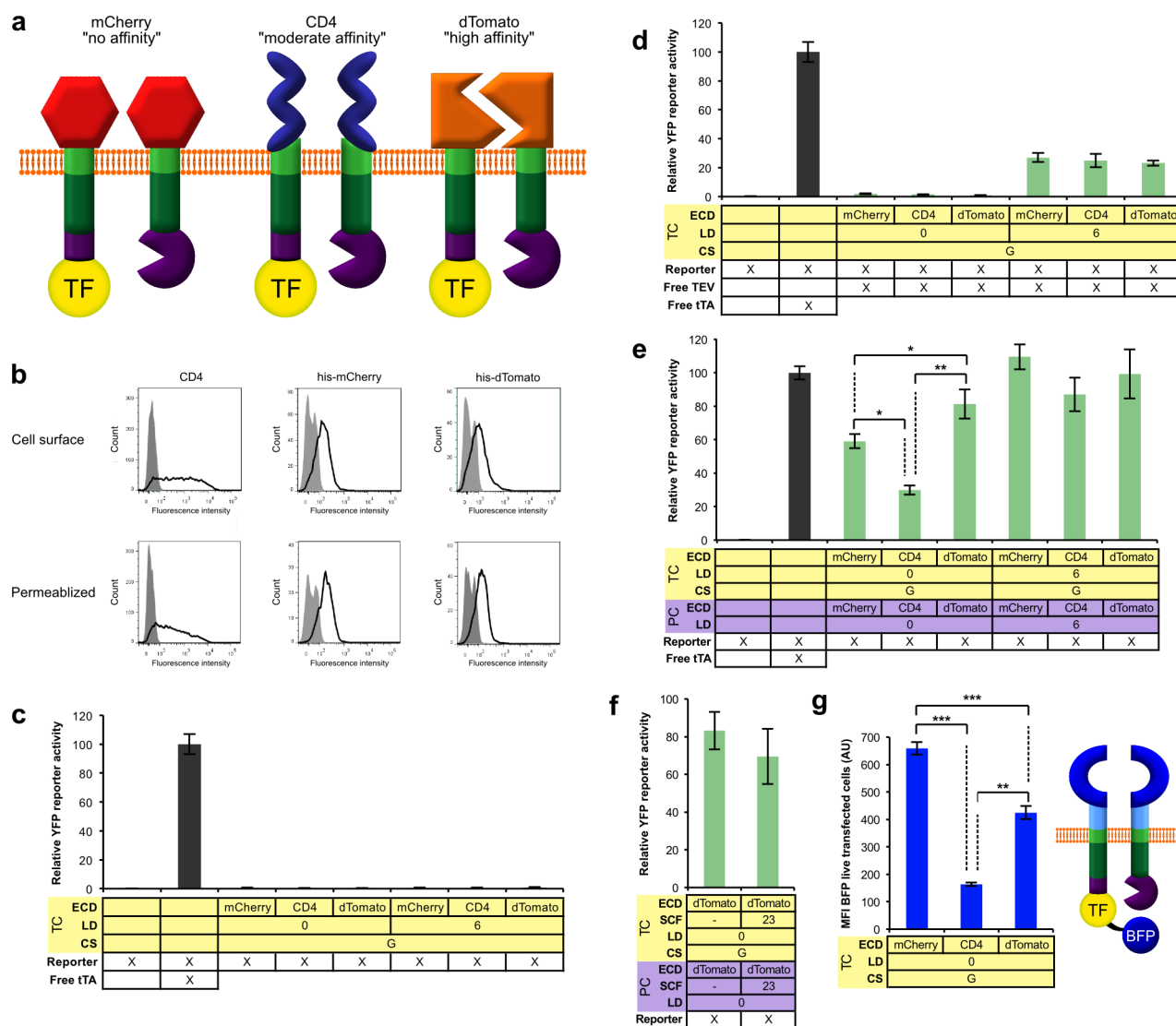
Figure 2. Evaluation of MESA concept using model receptors. (a) Schematic of model MESA based upon mCherry, CD4, and dTomato ectodomains. (b) Cell-surface and permeabilized (total) expression of 6xHis-tagged mCherry, 6xHis-tagged dTomato, and CD4 MESA was quantified via immunolabeling and flow cytometry (see Methods). Shaded region represents isotype control. (c−e) Reporter activity was measured for (c) target chains (TC) alone, (d) TC coexpressed with free cytosolic TEV, and (e) TC coexpressed with protease chains (PC). (f) Reporter activation by dTomato model MESA including a long (23 amino acid) flexible extracellular scaffold. (g) Relative expression of model MESA quantified using BFP-tTA fusion system (cartoon on the right). Experiments were conducted in biological triplicate, mean fluorescence intensity (MFI) of YFP was measured for each sample after gating on transfected cells, measurements were normalized relative to the internal control, and error bars represent the scaled standard deviation. (*$p \leq 0.05$, **$p \leq 0.01$, ***$p \leq 0.001$).

tion was mediated by interactions between receptor ectodomains and did not involve any ligands (Figure 2a). For these model receptors, ectodomains were derived from (a) mCherry, a monomeric fluorescent protein,[25] (b) CD4, which homodimerizes with a K_D of 1 mM (in solution),[26] or (c) dTomato, a fluorescent protein that is of comparable size to mCherry but that exists as an obligate homodimer, such that dTomato dimerization is essentially irreversible.[27] Thus, in this model system, the mCherry MESA represent monomeric receptors, which only encounter one another transiently due to diffusion within the cell membrane. Similarly, the CD4 MESA represent receptors that weakly dimerize, and the dTomato MESA represent receptors that strongly dimerize. Therefore, by comparing the amount of reporter gene activation conferred by mCherry MESA versus dTomato MESA having identical intracellular architectures, we can assess the degree to which

that particular intracellular architecture confers dimerization-dependent signaling. Hereafter, this differential activation of the reporter gene is described as "fold induction". We note that such model receptors should be capable of both heterotypic (TC-PC) and homotypic (PC-PC or TC-TC) dimerization, such that some dimers will be nonproductive, but this fact should not impair the use of these model MESA for comparative analysis of intracellular architectures.

The remainder of this initial MESA system was constructed as follows. To simplify preliminary design evaluations, no additional extracellular scaffold (SCF) was inserted. Transmembrane domains derived from CD28 were utilized to mediate cell surface expression of MESA, which is an approach used extensively for this purpose in fusion proteins such as chimeric antigen receptors (CAR).[12−16] Linker domains comprised flexible glycine/serine spacers of various lengths.

The autolysis-resistant tobacco etch virus protease S219 V mutant[28] (hereafter, TEV) and its wild type cleavage sequence (ENLYFQ/G) were selected as trans-cleavage partners based upon the specificity of this system and its extensive use in mammalian cells.[20,22,29] As indicated by a forward slash in the protease cleavage sequence above, cleavage occurs between glutamine and glycine residues, and the position following the slash is termed P1′. All constructs utilized the tet transactivator (tTA) as a constitutively active transcription factor, such that release of tTA from the plasma membrane induced expression of YFP from a tTA-responsive reporter construct.[30,31] All characterization experiments to follow included samples in which tTA was expressed from a plasmid to serve as an internal control that enables quantitative comparisons between independent experiments, and this "Free tTA" case does not necessarily represent maximal reporter gene activation.

We first investigated whether MESA constructs were expressed, localized to the cell surface, and signaled in a cleavage-dependent fashion. Each model MESA was expressed in HEK293FT cells by transient transfection, and cell surface expression of MESA was confirmed by flow cytometry (Figure 2b). When expressed alone, the target chains did not induce reporter activation (Figure 2c), but when target chains were coexpressed with free cytosolic TEV, increased reporter activation was detected (Figure 2d). TEV-dependent reporter activation increased when a 6-amino acid linker domain (LD) was inserted between the transmembrane and cleavage sequence domains of the target chain, perhaps due to increased accessibility of the cleavage sequence to TEV. Together, these data indicate that TEV-mediated cleavage of the target chain conferred tTA release, as expected.

To investigate how intracellular architecture and dimerization state impact MESA signaling, the various target chains and protease chains were coexpressed (Figure 2e). Overall, reporter activation was greater when target chains were coexpressed with protease chains rather than with cytosolic TEV, most likely because localization of TEV to the plasma membrane (as part of a protease chain) effectively increased the local concentration of TEV near the target chains. Similarly, dimerization-dependent reporter activation was observed only when the linker domain on the target chain was omitted; dTomato MESA induced significantly more reporter activation than did mCherry MESA ($p \leq 0.05$). We hypothesized that removing these linkers may geometrically constrain TEV and/or induce some steric hindrance due to proximity of the cleavage sequence to the plasma membrane, such that these constraints limit the probability of trans-cleavage during transient diffusive encounters between receptor chains but do not preclude trans-cleavage when target and protease chains dimerize. This hypothesis is supported by the observation that background decreased and fold induction increased when protein expression levels were decreased by transfecting lower amounts of the relevant expression vectors (Supporting Information). Importantly, even when dTomato domains were separated from transmembrane domains by long (23 amino acid) flexible extracellular scaffolds, reporter activation was not reduced (Figure 2f). Therefore, induction of MESA signaling requires only receptor dimerization (i.e., high local concentration of receptor chains), and the observed signaling is not dependent upon geometric peculiarities of the model MESA receptors. Moreover, this observation supports our technology development strategy in which intracellular architectures exhibiting robust dimerization-dependent signaling in model MESA are

subsequently coupled to various mechanisms for conferring ligand-induced receptor dimerization.

Based upon interchain affinities, CD4 MESA were predicted to induce reporter activation intermediate to that conferred by mCherry and dTomato constructs, but surprisingly, CD4MESA-mediated reporter activation was lowest of the three (Figure 2e). To investigate whether this pattern arose due to differences in MESA expression levels, BFP was genetically fused to the C-terminus of tTA on each target chain, enabling estimation of relative expression levels for each MESA through measurement of mean fluorescence intensity (MFI) of BFP using flow cytometry (Figure 2g). This analysis confirmed that CD4 MESA expression was lower than that of mCherry and dTomato MESA, and moreover, mCherry MESA expression was higher than that of dTomato MESA. This suggests that dimerization-dependent fold induction would be higher if the MESA were expressed at equal levels, which is most comparable to the target case of ligand-inducible MESA signaling. Therefore, this BFP fusion approach was used to account for differences in MESA expression levels and "correct" relative reporter activity in subsequent experiments (where indicated).

MESA Performance Optimization through Design-Based Tuning. Having demonstrated dimerization-dependent signaling, we next sought to improve performance characteristics (i.e., low background and large fold induction) by tuning MESA kinetics using a design-based approach. For example, background signaling is due to trans-cleavage during transient, diffusive receptor encounters. Thus, we hypothesized that background could be reduced by decreasing the affinity with which TEV binds its cleavage sequence (i.e., increasing K_M) and/or by reducing the rate at which cleavage occurs once TEV has bound its cleavage sequence (i.e., decreasing k_{cat}), such that the probability of trans-cleavage occurring during a transient encounter is reduced. Note that interactions between MESA ectodomains do not impact K_M, which is an intrinsic characteristic of the protease−substrate interaction. However, these modifications might also decrease total reporter output or decrease the dynamic range, such that various design objectives might be coupled. To explore these trade-offs, previously characterized variations in the P1′ residue of the cleavage sequence were introduced to "scan through" kinetic space.[32] To decouple the effects of modulating K_M or k_{cat}, variants were selected to individually modulate each parameter relative to a base case, and two such sets of three variants were constructed (Figure 3b). Varying k_{cat} generated large differences in both background and dimerization-induced reporter activation, and these trends were not explained by relatively small differences in MESA expression levels (Figure 3a,c). Strong reporter activation was only observed for cleavage sequences with large k_{cat}. Cleavage sequences with low k_{cat} had low overall reporter activation whether TEV bound weakly (large K_M) or strongly (small K_M) to its cleavage sequence but resulted in a higher fold induction than those with high k_{cat}. For sequences with large k_{cat} (those with serine (S), glycine (G), or alanine (A) in the P1′ position), the sequence with lowest K_M (the serine sequence) exhibited highest background. Thus, stronger binding of TEV to its cleavage sequence may increase the probability of trans-cleavage during transient encounters by stabilizing the protease−substrate interaction. As was observed with earlier constructs, fold induction was higher when accounting for differences in MESA expression levels (Figure 3d). Finally, for all cleavage sequences explored, no
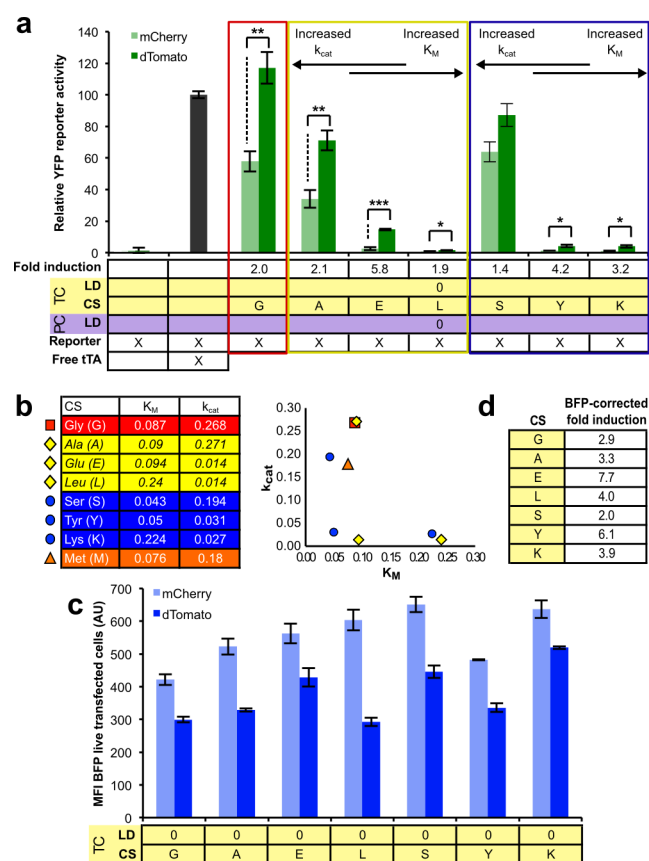
Figure 3. Tuning MESA cleavage kinetics via cleavage sequence variants. (a) Reporter activity cleavage sequence P1′ position variants. (b) K_M and k_{cat} reported for selected P1′ variants.[32] (c) Fold induction "corrected" for relative MESA expression levels. (d) BFP expression levels used to generate corrected metrics in (c). Refer to Figure 2 for measurement details. (*$p \leq 0.05$, **$p \leq 0.01$, ***$p \leq 0.001$).

Figure 4. Design-based optimization of MESA performance. (a) Evaluation of methionine (M) cleavage sequence and truncated TEV (tTEV) design variants. (b) Fold induction "corrected" for relative MESA expression levels. (c) BFP expression levels used to generate corrected metrics in panel b. Refer to Figure 2 for measurement details. (*$p \leq 0.05$, **$p \leq 0.01$, ***$p \leq 0.001$).

dimerization-inducible activity was observed for MESA containing a 6 amino acid linker (Supporting Information), indicating that the steric occlusion conferred by removing the linker is required to tune cleavage kinetics to enable robust dimerization-dependent signaling.

This kinetic exploration suggested several strategies for improving receptor performance. First, we postulated that a cleavage sequence with large K_M and moderate k_{cat} might both decrease background and increase fold induction. To test this hypothesis, a cleavage sequence with methionine (M) at P1′ was utilized (Figure 3b). Fold induction was improved from 1.9 for the wild type (G) cleavage sequence to 2.4 for M cleavage sequence (Figure 4a). When corrected for variations in MESA expression levels, fold induction was 3.0 and 5.8 for the G and M cleavage sequences, respectively (Figure 4b, c). We then hypothesized that further increases in K_M without decreasing k_{cat} could further improve MESA performance. Since none of the cleavage sequences characterized by Kapust et al. combined high K_M with a moderate or high k_{cat},[32] a previously reported truncated TEV (tTEV) variant that increases K_M without affecting k_{cat}[28] was investigated (Figure 4a,b). Expression-corrected fold induction increased from 3.0 with full-length TEV to 3.7 with truncated TEV for the G cleavage sequence, and from 5.8 to 8.3, respectively, for the M cleavage sequence. Notably, combining the M cleavage sequence with tTEV resulted in large fold induction but small total reporter activation, again indicating the existence of design trade-offs
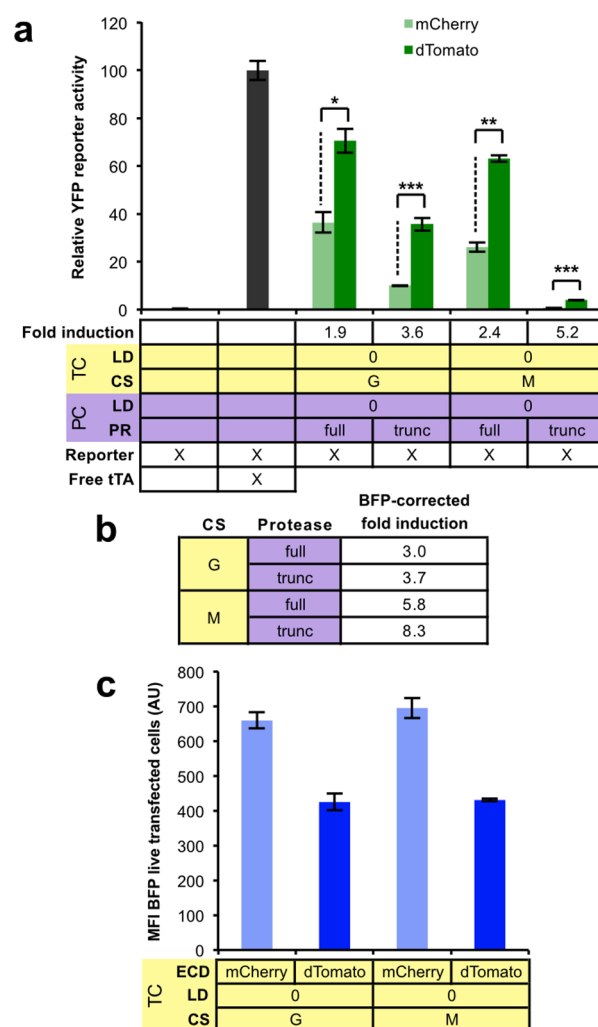
that can be weighed and tuned to suit a particular application. Having thus identified multiple intracellular MESA architectures that confer dimerization-dependent signaling in model receptors, we next investigated whether these findings enable construction of ligand-inducible receptors.

Ligand-Inducible MESA Signaling. To test our hypothesis that the challenge of achieving ligand-induced dimerization may be decoupled from the challenge of achieving dimerization-induced signaling, functional intracellular domains identified using model MESA receptors were genetically fused to extracellular domains that heterodimerize in the presence of the small molecule rapamycin: FKBP (FK506-binding protein of 12 kDa) and FRB (FKBP rapamycin-binding).[33] These rapamycin-binding domains have been used for many applications including ligand-induced protein splicing[34−36] and regulation of gene expression.[37−39] The two domains do not interact in the absence of rapamycin, and upon the addition of rapamycin, a stable tertiary complex forms with $K_d \approx 2.5$ nM.[33,40] Two sets of MESA were created, in which either the FRB or FKBP domain was fused to either the protease chain or the target chain. All receptors included the G protease cleavage sequence

(TC) or full length TEV (PC), and a two amino acid linker comprising the extracellular scaffold linking the transmembrane domain to FRB or FKBP. We chose to initially characterize the rapamycin MESA receptors using the wild type (G) cleavage sequence in order to achieve a maximal level of reporter activation to facilitate detection, and we expected that this choice might come at the expense of high background signaling.

As observed with previous receptors (Figure 2c), no single MESA chain induced reporter activity (± rapamycin) (Figure 5a). Background was also very low for complementary pairs of
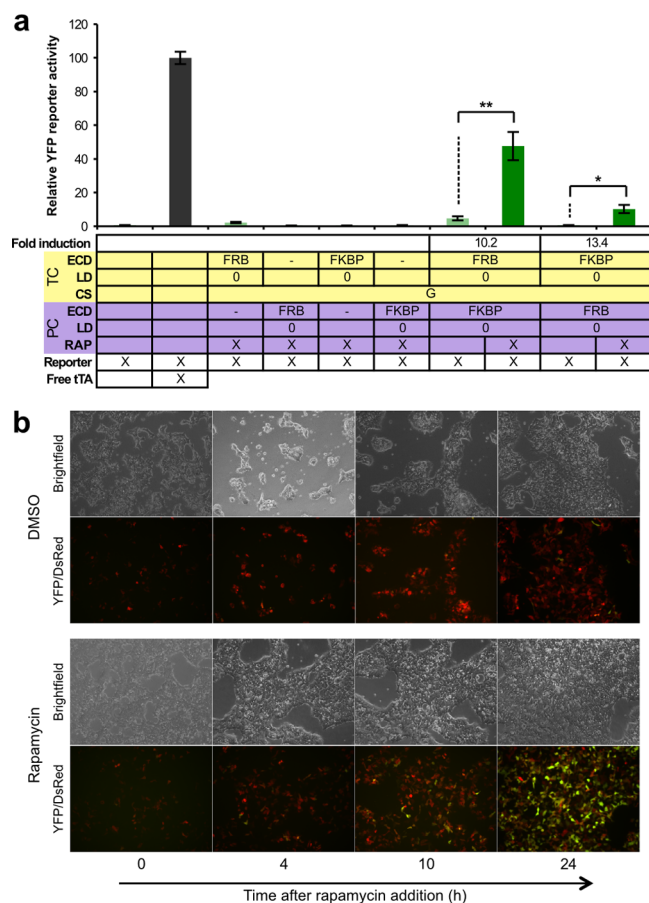

Figure 5. Ligand binding-inducible MESA signaling. (a) Measurement of reporter activation for rapamycin MESA constructs with (dark green) and without (light green) addition of rapamycin. (b) Fluorescent micrographs illustrating rapamycin-induced MESA reporter activation over time. Yellow (YFP) represents reporter activation, and red (DsRedExpress2) is a transfection control. Refer to Figure 2 for measurement details and see text for abbreviations. (*$p \leq 0.05$, **$p \leq 0.01$, ***$p \leq 0.001$).

MESA (e.g., FRB on TC and FKBP on PC or vice versa), and after rapamycin addition, reporter activation was observed within 10 h and increased over 24 h (Figure 5a,b). The concentration of rapamycin used for this experiment (100 nM) was selected to be consistent with previous work using rapamycin-binding domains for protein–protein interactions.[34−36] Reporter activation was highest when the FRB domain was on the TC (fold induction = 10.2), but the background was lowest when the FRB domain was on the PC, and therefore, the fold induction was greater (fold induction = 13.4). Given the high background observed for model MESA using the G cleavage sequence, the low background observed

for the rapamycin binding constructs was surprising and may be partially explained by the lower expression of rapamycin MESA chains (Supporting Information). The fold induction upon ligand addition is likely enhanced by the fact that unlike our model MESA, the rapamycin MESA heterodimerize rather than homodimerize and therefore do not form nonproductive dimers. This successful generation of ligand-inducible MESA confirms that this modular receptor architecture can be coupled with general systems for achieving ligand-induced dimerization to generate biosensors for exclusively extracellular ligands.

Additional MESA Output Modality: Enzyme Reconstitution. Although the basic MESA mechanism (Figure 1) is well-suited to coupling MESA output to the regulation of genetic circuits, we next designed MESA receptors in which receptor dimerization alters cell state via a transcription-independent mechanism: reconstitution of enzymatic activity. In this system, N- and C-terminal fragments of TEV were each fused to separate MESA chains, such that ligand binding-induced dimerization should promote reconstitution of split TEV protease (sTEV), which can be monitored by cleavage of a third "target" chain (Figure 6a). Split TEV has been used to monitor protein−protein interactions,[22] and this concept appears to be generalizable to reconstitution of many proteins, as similar systems using split GFP,[21,41,42] split luciferase,[43] or split beta-lactamase[44,45] have been developed. Hypothetically, MESA−induced activation of enzymatic activity could couple biosensing to metabolism, could enable MESA-mediated control of processes in enucleated cells, or could rapidly induce physiological processes such as caspase-induced apoptosis. Thus, reconstitution of sTEV serves as a proof of principle for a wide range of potential MESA outputs. We also hypothesized that sTEV-MESA might exhibit low background and improved signal-to-noise, since diffusive encounters between partial TEV fragments and the target chain would not result in a cleavage event.

Because the sTEV-MESA utilize a different mechanism of activation than do the basic MESA, we performed an independent characterization of this design space. An initial library of sTEV MESA variants was generated in which dTomato or mCherry ectodomains again served as model receptors, and 6 or 12 residue intracellular linker domains were initially included on each chain because we anticipated that extra flexibility might be required to allow protease reconstitution. The TEV protease was split into N- and C-terminal fragments to partition the enzyme's active site:[22] amino acid residues 1−118 (NTEV) on the protease chain with NTEV (PC_N) and residues 119−242 (CTEV) on the protease chain with CTEV (PC_C) (Figure 6a). A library of target chains was also generated in which mCherry served as the ectodomain and various linkers and cleavage sequences separated the transmembrane domain from tTA. None of the target chains induced reporter activation in the absence of TEV, and since the target chain with G cleavage sequence and 6 amino acid linker signaled most strongly when coexpressed with soluble TEV (Figure 6b), this construct was initially selected for evaluating the sTEV MESA concept. This target chain was coexpressed with sTEV PC_N or PC_C individually, confirming that neither sTEV chain alone induced detectable cleavage of the target chain (Figure 6c). When the target chain was coexpressed with surface-bound TEV (sb TEV; a mCherry protease chain from the basic MESA system, Figure 1, with a zero residue LD), reporter activation was evident. However, when monomeric mCherry-based PC_N and PC_C were coex-
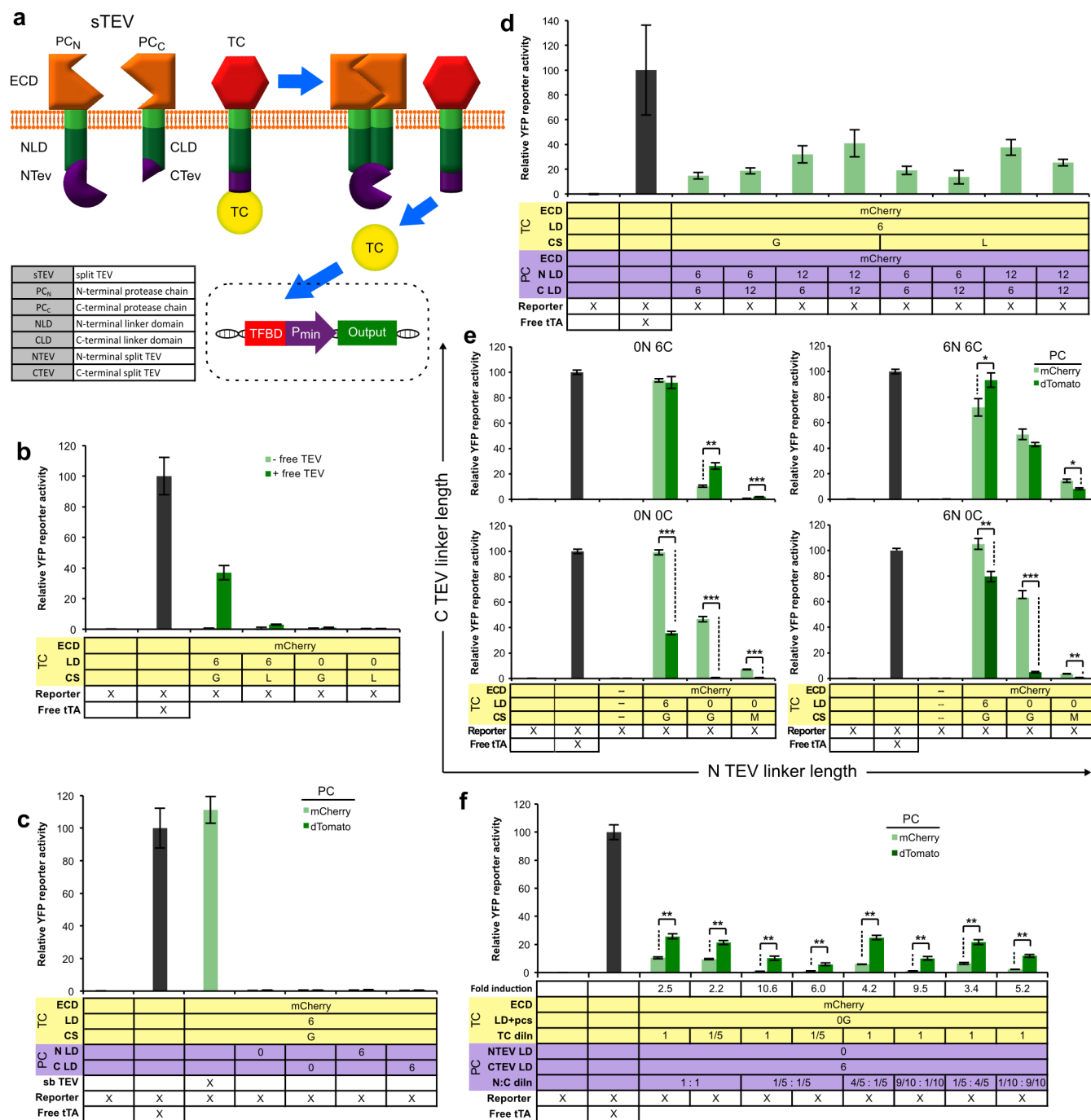
Figure 6. MESA-regulated enzyme reconstitution. (a) Components and proposed mechanism for the split TEV (sTEV) MESA system. (b) Cleavage of target chain variants by cytosolic TEV. (c) Individual split TEV fragments lack proteolytic activity. (d) Geometric and kinetic analysis of contributors to sTEV background. (e) Contributions of linker length and cleavage kinetics to dimerization-inducible sTEV MESA signaling. (f) Effects of receptor stoichiometry on sTEV MESA performance. For target chain dilutions, fractions are defined relative to the starting amount of 1 μg of target chain plasmid vector DNA per sample, with empty vector plasmid used to keep the total amount of DNA transfected constant. For protease chain dilutions, fractions are again defined relative to the starting amount (1 μg each of PC_N and PC_C plasmid vectors), and empty vector plasmid was again used to keep the total amount of DNA transfected constant. Refer to Figure 2 for measurement details. (*$p \leq 0.05$, **$p \leq 0.01$, ***$p \leq 0.001$).

pressed, cleavage of target chains bearing either the most or least kinetically favorable cleavage sequences (G and L, respectively) was also observed (Figure 6d). These data indicate that diffusive encounters were sufficient to reconstitute sTEV in these constructs (which we term, "spontaneous sTEV reconstitution"). Since Wehr et al. did not observe spontaneous reconstitution of sTEV in membrane-bound constructs,[22] we

hypothesized that this difference could be due to expression level differences or our inclusion of long (6 or 12 amino acid) unstructured linkers that facilitate sTEV refolding (Wehr et al. omitted such linkers).

To investigate strategies for reducing target chain cleavage due to spontaneous sTEV reconstitution, a library of sTEV variants was constructed including linkers of 0 or 6 amino acids,

and these were coexpressed with target chains including G or M cleavage sequences and linkers of 0 or 6 amino acids. For PC_C with 0 linkers, reporter activity was "de-inducible" upon dimerization for all target chains (Figure 6e). To explain this phenomenon, we hypothesized that dTomato-mediated dimerization of ectodomains may cause the protease chains to dimerize in a conformation that precludes refolding of sTEV fragments, whereas the freely diffusing mCherry constructs may have sufficient geometric freedom to permit reconstitution following diffusive encounter. Receptors with 6 residue linkers on both PCs exhibited dimerization-independent reporter activation, potentially due to spontaneous sTEV reconstitution during transient diffusive encounters. However, when the PC_N lacking intracellular linkers and the PC_C with 6 residue linkers were coexpressed with a target with 0 linkers and the G cleavage sequence, a 2.5 fold induction upon dimerization was observed. Although it is certainly possible that fold induction could be further increased by refinement of this scenario (e.g., by considering target chain linker lengths between 0 and 6 amino acids), optimization of these constructs was not the objective of this proof of principle investigation, and we opted to further characterize this functional architecture.

Because each sTEV MESA signaling event requires interaction between three receptor chains, we investigated how varying the stoichiometry of sTEV MESA components would impact signaling (Figure 6f). While reducing the quantity of target chain transfected did not appreciably affect fold induction, reducing the quantity of both PC_N and PC_C transfected increased fold induction from 2.5 to 10.6. Similarly, reducing the amount of *either* PC_N or PC_C transfected also increased fold induction to an intermediate degree. Together, these data demonstrate that this mechanism for achieving dimerization-dependent signaling is robust to variations in relative MESA expression levels, and fold induction may be optimized by tuning the expression of protease chains to limit spontaneous sTEV reconstitution. Thus, reconstitution of enzymatic activity provides an additional modality for coupling MESA biosensing to regulation of cell state.

Ligand-Inducible Enzyme Reconstitution. We next investigated whether the sTEV MESA mechanism could be harnessed to achieve ligand-inducible enzyme reconstitution. Thus, sTEV MESA chains were constructed in which the heterodimeric rapamycin binding domains (FRB and FKBP) were utilized as ectodomains for the protease chains. Based upon results from model sTEV MESA (Figure 6), we evaluated PC_N with 0 and 6 linkers and PC_C with 6 linkers, since PC_C with 0 linkers appeared incompatible with sTEV reconstitution. A flexible scaffold (2 or 6 amino acids) was also inserted between transmembrane and rapamycin-binding domains on the protease chains, because we hypothesized that some flexibility would be required to enable simultaneous dimerization of rapamycin-binding domains and reconstitution of sTEV fragments. Since the geometric constraints governing the mobility of reconstituted sTEV may differ when protease chain dimerization is mediated by rapamycin-binding domains vs dTomato domains (used in Figure 5), we investigated target chains including either 0 or 6 amino acid intracellular linkers and a G cleavage sequence. In control experiments, rapamycin-sTEV MESA performed similarly to model sTEV MESA—no signaling was observed when the target chain was expressed alone or paired with only PC_C or PC_N (Supporting Information).

When this small library of potential receptors was functionally evaluated, several configurations exhibited significant rapamycin-inducible signaling (Figure 7). The highest fold
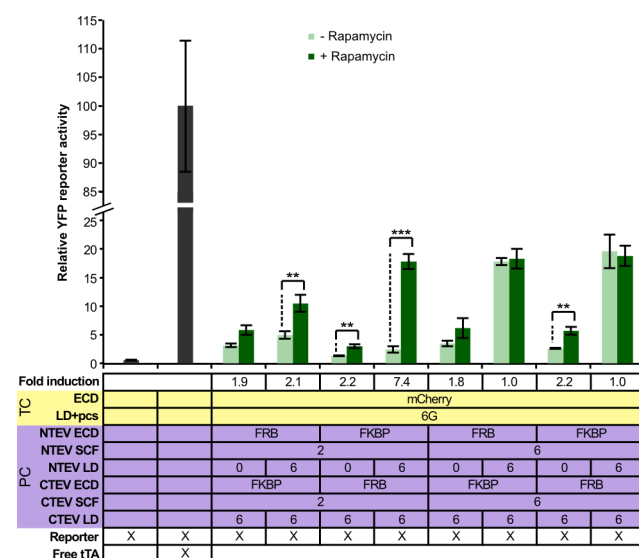
			1.9	2.1	2.2	7.4	1.8	1.0	2.2	1.0
Fold induction			1.9	2.1	2.2	7.4	1.8	1.0	2.2	1.0
TC — ECD			mCherry							
TC — LD+pcs			6G							
PC — NTEV ECD			FRB		FKBP		FRB		FKBP	
PC — NTEV SCF			2				6			
PC — NTEV LD			0	6	0	6	0	6	0	6
PC — CTEV ECD			FKBP		FRB		FKBP		FRB	
PC — CTEV SCF			2				6			
PC — CTEV LD			6	6	6	6	6	6	6	6
Reporter	X	X	X	X	X	X	X	X	X	X
Free tTA		X								

Figure 7. Ligand-inducible enzyme reconstitution. Reporter activation was measured for rapamycin sTEV MESA expressed transiently in cells cultured without rapamycin (light green) or with rapamycin (dark green). Refer to Figure 2 for measurement details. ($*p \leq 0.05$, $**p \leq 0.01$, $***p \leq 0.001$).

induction (7.4) was observed for receptors with 2 extracellular scaffold linkers, and 6 intracellular linkers on both the PC_N (FKBP) and PC_C (FRB). However, no rapamycin-inducible signaling was observed when these protease chains were expressed with target chains lacking an intracellular linker (Supporting Information). This suggests that rapamycin-mediated sTEV reconstitution resulted in protease chain complexes to which the linker-less target chain was sterically or geometrically inaccessible. Although the number of design variations considered in this experiment was limited, one general trend may be that inducible receptor configurations involved a combination of protease chain linker lengths that somewhat constrained receptor flexibility and potentially limited spontaneous sTEV reconstitution.

It may well be possible to further optimize receptor performance by modifying the promising constructs reported here (e.g., by considering intermediate linker lengths). Importantly, this design space may be explored by making such rational changes to the initial constructs characterized here. Overall, this proof of principle experiment demonstrates that the MESA platform may be adapted to engineer novel ligand-inducible receptor output modalities.

Conclusions and Future Prospects. The MESA platform addresses a key technological gap in the mammalian synthetic biology toolbox and will enable robust interfacing of engineered cell-based devices with host physiology. Moreover, this investigation demonstrates the feasibility of engineering integrated receptors and signal transduction systems from the ground up using modular components, and this novel approach may well be extended to engineering biosensor systems in other cellular contexts, potentially including microbial hosts.

Although the initial MESA development described here relied upon design-based methods, it is certainly possible that these functional designs may serve as starting points for further

optimization using approaches such as directed evolution or computation-guided protein engineering. In general, the MESA platform enables design-based receptor engineering because it is possible to tune specific biophysical parameters by modifying the sequence of specific receptor domains. In this investigation, we made use of this property to identify functional receptor designs via limited trial-and-error searches. In the future, this property of tunability may be further leveraged to develop predictive design tools. MESA development was conducted using transient transfection in order to identify architectures that are likely to signal robustly in many contexts and over various expression levels. In particular, our data suggest that stable receptor expression via lentiviral transduction or stable integration of expression vectors into safe harbors in host chromosomal DNA should result in both lower background and greater fold induction (Supporting Information).

The quantitative exploration of design space presented here also provides a framework for readily adapting MESA technology to novel inputs (ligands), outputs (transcription factors or enzymes), and applications of interest. For example, MESA output may be amplified by coupling it to gene circuits such as positive feedback amplifiers.[46] Because MESA signaling is self-contained, it should also be possible to multiplex MESA receptors (e.g., using multiple engineered transcription factors as outputs). Coupling multiplexed receptors to novel or existing logic-based gene circuits[6,8,47] should enable novel capabilities including multiparametric evaluation of extracellular ligands. MESA could be used in combination with other sensor-effector systems such as CAR technologies to increase the safety and efficacy of cell-based immunotherapy.[19] As mammalian synthetic biology plays an increasingly important role in clinical applications, platform technologies such as MESA are needed to construct complex and customizable cell-based devices that enable new and effective therapeutic strategies.

■ METHODS

DNA Constructs. Constructs encoding MESA fusion proteins were assembled by PCR amplification and standard molecular cloning. MESA constructs were cloned into the adeno-associated virus expression vector plasmid pAAV GFP SN,[48,49] although expression was achieved by transient transfection (not viral packaging). pDSRedExpress2 was included as a transfection control. Source plasmids for MESA components included pCL-CTIG (Addgene plasmid 14901),[50] pRK1043 (Addgene plasmid 8835),[28] pBI-MCS-EGFP (Addgene plasmid 16542),[31] pBS mCD4 (Addgene plasmid 14613),[51] AAV-FLEX-rev-ChR2-tdtomato (Addgene plasmid 18917),[52] pEBFP2-Nuc (Addgene plasmid 14893),[53] YFP-FKBP (Addgene plasmid 20175)[54] and YFP-tagged FRB (YR) (Addgene plasmid 20148),[54] pmCherry-C1 (Clontech 632524).[27] A complete list of DNA constructs as well as plasmids and primers used for cloning can be found in Supporting Information.

Cell Culture and Transfection. HEK293FT cells (Life Technologies) were maintained at 37 °C in 5% CO_2 in growth medium (Dulbecco's modified growth medium supplemented with 10% FBS, 1% penicillin–streptomycin, and 4 mM L-glutamine). Transfections were performed in 10 cm plates seeded with 6×10^6 cells in 10 mL media (for immunochemistry) or in 24 well plates seeded with 1.5×10^5 cells in 0.5–0.75 mL media (for receptor signaling experiments). Cells were seeded 8–12 h before transfection by the $CaCl_2$–HEPES-buffered saline (HeBS) method. For rapamy-

cin-induced signaling experiments, media change occurred 16 h post-transfection at which time rapamycin (Santa Cruz Biotechnology Inc., 100 nM with 0.5% DMSO, final concentrations) or DMSO (0.5% final concentration) was added to culture media, and cells were incubated for 24 h before analysis.

Flow cytometry. Approximately 1×10^4 live cells from each transfected well were analyzed using an LSRII flow cytometer (BD Bioscience) running FACSDiva software. Cells were harvested 36 h post-transfection by trypsinization with 0.15 mL trypsin-EDTA or PBS with 0.5 mM EDTA and resuspended in phosphate buffered saline (PBS) with 5% bovine serum albumin (BSA) and 0.5 mM EDTA to prevent formation of aggregates. Data were electronically compensated and analyzed using FlowJo software (Tree Star). Live single cells were gated based on scatter, and DsRedExpress2+ cells were gated as "transfected," and reporter activity (YFP) was quantified and normalized with respect to the internal control (reporter plasmid + constitutively expressed tTA). Example gating is included in Supporting Information. Samples were collected and analyzed in biological triplicate, and data points and error bars represent the mean and standard deviation, respectively, of the mean fluorescent intensity measured for each biological replicate.

Immunolabeling. Cells transfected with CD4 MESA or N-terminal 6xHis-tagged mCherry or dTomato MESA (no reporter plasmid) were harvested as previously described, fixed in 2% paraformaldehyde in PBS, and either left intact for surface labeling or permeabilized in PWB buffer (0.5% saponin, 0.2% BSA in PBS) for whole-cell labeling. Cells transfected with 6xHis-tagged constructs were incubated with fluorescein isothiocyanate (FITC)-conjugated rabbit polyclonal antibodies against the 6xHis tag (ab1206 from Abcam), or a FITC-conjugated rabbit IgG isotype control (ab37406 from Abcam) to control for nonspecific binding. FITC expression was quantified by flow cytometry and analyzed as previously described, with mCherry or dTomato on MESA chains serving as the transfection control for gating. CD4 construct-transfected cells were incubated with phycoerythrin (PE) conjugated rat antimouse CD4 antibodies (#100408 from BioLegend) or PE-conjugated isotype control (#400607 from BioLegend).

■ ASSOCIATED CONTENT

ⓢ Supporting Information

Supplemental figures, complete methods (including Excel sheet of primers and demonstrations of flow cytometry analysis), and GenBank sequence files of representative constructs. This information is available free of charge via the Internet at http://pubs.acs.org

■ AUTHOR INFORMATION

Corresponding Author

*E-mail: j-leonard@northwestern.edu.

Author Contributions

N.M.D., R.M.D., K.A.S., and J.N.L. designed and analyzed experiments; N.M.D., R.M.D., and K.A.S. conducted experiments; and N.M.D., R.M.D., K.A.S., and J.N.L. wrote the manuscript.

Notes

The authors declare the following competing financial interest: A U.S. patent application covering inventions described in this manuscript has been filed.

■ ABBREVIATIONS

TC, target chain; PC, protease chain; TF, transcription factor; ECD, ectodomain; SCF, extracellular scaffold; LD, intracellular linker domain; CS, cleavage sequence; PR, protease; tTA, Tet transactivator; TEV, tobacco etch virus (protease); sTEV, split TEV; RAP, rapamycin; PC_N, protease chain with N-terminal split TEV; PC_C, protease chain with C-terminal split TEV; NLD, intracellular linker on PC_N; CLD, intracellular linker on PC_C; NTev, N-terminal portion of split TEV; CTev, C-terminal portion of split TEV

■ REFERENCES

(1) Weber, W., Bacchus, W., Daoud-El Baba, M., and Fussenegger, M. (2007) Vitamin H-regulated transgene expression in mammalian cells. *Nucleic Acids Res. 35*, e116.

(2) Weber, W., Lienhart, C., Baba, M. D., and Fussenegger, M. (2009) A biotin-triggered genetic switch in mammalian cells and mice. *Metab Eng 11*, 117−124.

(3) Fung, E., Wong, W. W., Suen, J. K., Bulter, T., Lee, S. G., and Liao, J. C. (2005) A synthetic gene-metabolic oscillator. *Nature 435*, 118−122.

(4) Weber, W., Daoud-El Baba, M., and Fussenegger, M. (2007) Synthetic ecosystems based on airborne inter- and intrakingdom communication. *Proc. Natl. Acad. Sci. U.S.A. 104*, 10435−10440.

(5) Wang, W. D., Chen, Z. T., Kang, B. G., and Li, R. (2008) Construction of an artificial intercellular communication network using the nitric oxide signaling elements in mammalian cells. *Exp. Cell Res. 314*, 699−706.

(6) Culler, S. J., Hoff, K. G., and Smolke, C. D. (2010) Reprogramming cellular behavior with RNA controllers responsive to endogenous proteins. *Science 330*, 1251−1255.

(7) Wright, C. M., Wright, R. C., Eshleman, J. R., and Ostermeier, M. (2011) A protein therapeutic modality founded on molecular regulation. *Proc. Natl. Acad. Sci. U.S.A. 108*, 16206−16211.

(8) Kramer, B. P., Fischer, M., and Fussenegger, M. (2005) Semi-synthetic mammalian gene regulatory networks. *Metab. Eng. 7*, 241−250.

(9) Xie, Z., Wroblewska, L., Prochazka, L., Weiss, R., and Benenson, Y. (2011) Multi-input RNAi-based logic circuit for identification of specific cancer cells. *Science 333*, 1307−1311.

(10) Armbruster, B. N., Li, X., Pausch, M. H., Herlitze, S., and Roth, B. L. (2007) Evolving the lock to fit the key to create a family of G protein-coupled receptors potently activated by an inert ligand. *Proc. Natl. Acad. Sci. U.S.A. 104*, 5163−5168.

(11) Conklin, B. R., Hsiao, E. C., Claeysen, S., Dumuis, A., Srinivasan, S., Forsayeth, J. R., Guettier, J. M., Chang, W. C., Pei, Y., McCarthy, K. D., Nissenson, R. A., Wess, J., Bockaert, J., and Roth, B. L. (2008) Engineering GPCR signaling pathways with RASSLs. *Nat. Methods 5*, 673−678.

(12) Finney, H. M., Lawson, A. D., Bebbington, C. R., and Weir, A. N. (1998) Chimeric receptors providing both primary and costimulatory signaling in T cells from a single gene product. *J Immunol 161*, 2791−2797.

(13) Hombach, A., Wieczarkowiecz, A., Marquardt, T., Heuser, C., Usai, L., Pohl, C., Seliger, B., and Abken, H. (2001) Tumor-specific T cell activation by recombinant immunoreceptors: CD3 zeta signaling and CD28 costimulation are simultaneously required for efficient IL-2 secretion and can be integrated into one combined CD28/CD3 zeta signaling receptor molecule. *J. Immunol. 167*, 6123−6131.

(14) Brentjens, R. J., Latouche, J. B., Santos, E., Marti, F., Gong, M. C., Lyddane, C., King, P. D., Larson, S., Weiss, M., Rivière, I., and Sadelain, M. (2003) Eradication of systemic B-cell tumors by genetically targeted human T lymphocytes co-stimulated by CD80 and interleukin-15. *Nat Med 9*, 279−286.

(15) Porter, D. L., Levine, B. L., Kalos, M., Bagg, A., and June, C. H. (2011) Chimeric antigen receptor-modified T cells in chronic lymphoid leukemia. *N. Engl. J. Med. 365*, 725−733.

(16) Kalos, M., Levine, B. L., Porter, D. L., Katz, S., Grupp, S. A., Bagg, A., and June, C. H. (2011) T cells with chimeric antigen receptors have potent antitumor effects and can establish memory in patients with advanced leukemia. *Sci. Transl. Med. 3*, 95ra73.

(17) Brentjens, R. J., Davila, M. L., Riviere, I., Park, J., Wang, X., Cowell, L. G., Bartido, S., Stefanski, J., Taylor, C., Olszewska, M., Borquez-Ojeda, O., Qu, J., Wasielewska, T., He, Q., Bernal, Y., Rijo, I. V., Hedvat, C., Kobos, R., Curran, K., Steinherz, P., Jurcic, J., Rosenblat, T., Maslak, P., Frattini, M., and Sadelain, M. (2013) CD19-targeted T cells rapidly induce molecular remissions in adults with chemotherapy-refractory acute lymphoblastic leukemia. *Sci. Transl. Med. 5*, 177ra138.

(18) James, J. R., and Vale, R. D. (2012) Biophysical mechanism of T-cell receptor triggering in a reconstituted system. *Nature 487*, 64−69.

(19) Dudek, R. M., Chuang, Y., and Leonard, J. N. (in press) Engineering cell-based therapies: a vanguard of design-driven medicine, In *A Systems Biology Approach to Blood* (Corey, S. J., Kimmel, M., and Leonard, J. N., Eds.) Springer, Heidelberg.

(20) Barnea, G., Strapps, W., Herrada, G., Berman, Y., Ong, J., Kloss, B., Axel, R., and Lee, K. J. (2008) The genetic design of signaling cascades to record receptor activation. *Proc. Natl. Acad. Sci. U.S.A. 105*, 64−69.

(21) Wilson, C. G., Magliery, T. J., and Regan, L. (2004) Detecting protein−protein interactions with GFP-fragment reassembly. *Nat. Methods 1*, 255−262.

(22) Wehr, M. C., Laage, R., Bolz, U., Fischer, T. M., Grünewald, S., Scheek, S., Bach, A., Nave, K. A., and Rossner, M. J. (2006) Monitoring regulated protein−protein interactions using split TEV. *Nat. Methods 3*, 985−993.

(23) Maeder, M. L., Thibodeau-Beganny, S., Sander, J. D., Voytas, D. F., and Joung, J. K. (2009) Oligomerized pool engineering (OPEN): An 'open-source' protocol for making customized zinc-finger arrays. *Nat. Protocols 4*, 1471−1501.

(24) Cermak, T., Doyle, E. L., Christian, M., Wang, L., Zhang, Y., Schmidt, C., Baller, J. A., Somia, N. V., Bogdanove, A. J., and Voytas, D. F. (2011) Efficient design and assembly of custom TALEN and other TAL effector-based constructs for DNA targeting. *Nucleic Acids Res. 39*, e82.

(25) Panter, G., and Jerala, R. (2011) The ectodomain of the Toll-like receptor 4 prevents constitutive receptor activation. *J. Biol. Chem. 286*, 23334−23344.

(26) Wu, H., Kwong, P. D., and Hendrickson, W. A. (1997) Dimeric association and segmental variability in the structure of human CD4. *Nature 387*, 527−530.

(27) Shaner, N. C., Campbell, R. E., Steinbach, P. A., Giepmans, B. N., Palmer, A. E., and Tsien, R. Y. (2004) Improved monomeric red, orange and yellow fluorescent proteins derived from *Discosoma sp.* red fluorescent protein. *Nat. Biotechnol. 22*, 1567−1572.

(28) Kapust, R. B., Tozser, J., Fox, J. D., Anderson, D. E., Cherry, S., Copeland, T. D., and Waugh, D. S. (2001) Tobacco etch virus protease: mechanism of autolysis and rational design of stable mutants with wild-type catalytic proficiency. *Protein Eng. 14*, 993−1000.

(29) Parks, T. D., Leuther, K. K., Howard, E. D., Johnston, S. A., and Dougherty, W. G. (1994) Release of proteins and peptides from fusion proteins using a recombinant plant virus proteinase. *Anal. Biochem. 216*, 413−417.

(30) Gossen, M., and Bujard, H. (1992) Tight control of gene expression in mammalian cells by tetracycline-responsive promoters. *Proc. Natl. Acad. Sci. U.S.A. 89*, 5547−5551.

(31) Yu, J., Zhang, L., Hwang, P. M., Rago, C., Kinzler, K. W., and Vogelstein, B. (1999) Identification and classification of p53-regulated genes. *Proc. Natl. Acad. Sci. U.S.A. 96*, 14517−14522.

(32) Kapust, R. B., Tozser, J., Copeland, T. D., and Waugh, D. S. (2002) The P1′ specificity of tobacco etch virus protease. *Biochem. Biophys. Res. Commun. 294*, 949−955.

(33) Bierer, B. E., Mattila, P. S., Standaert, R. F., Herzenberg, L. A., Burakoff, S. J., Crabtree, G., and Schreiber, S. L. (1990) Two distinct signal transmission pathways in T lymphocytes are inhibited by complexes formed between an immunophilin and either FK506 or rapamycin. *Proc. Natl. Acad. Sci. U.S.A. 87*, 9231−9235.

(34) Selgrade, D. F., Lohmueller, J. J., Lienert, F., and Silver, P. A. (2013) Protein scaffold-activated protein trans-splicing in mammalian cells. *J. Am. Chem. Soc. 135*, 7713−7719.

(35) Mootz, H. D., Blum, E. S., Tyszkiewicz, A. B., and Muir, T. W. (2003) Conditional protein splicing: A new tool to control protein structure and function *in vitro* and *in vivo*. *J. Am. Chem. Soc. 125*, 10561−10569.

(36) Schwartz, E. C., Saez, L., Young, M. W., and Muir, T. W. (2007) Post-translational enzyme activation in an animal via optimized conditional protein splicing. *Nat. Chem. Biol. 3*, 50−54.

(37) Ho, S. N., Biggar, S. R., Spencer, D. M., Schreiber, S. L., and Crabtree, G. R. (1996) Dimeric ligands define a role for transcriptional activation domains in reinitiation. *Nature 382*, 822−826.

(38) Schlatter, S., Senn, C., and Fussenegger, M. (2003) Modulation of translation-initiation in CHO-K1 cells by rapamycin-induced heterodimerization of engineered eIF4G fusion proteins. *Biotechnol. Bioeng. 83*, 210−225.

(39) Rivera, V. M., Clackson, T., Natesan, S., Pollock, R., Amara, J. F., Keenan, T., Magari, S. R., Phillips, T., Courage, N. L., Cerasoli, F., Jr., Holt, D. A., and Gilman, M. (1996) A humanized system for pharmacologic control of gene expression. *Nat. Med. 2*, 1028−1032.

(40) Banaszynski, L. A., Liu, C. W., and Wandless, T. J. (2005) Characterization of the FKBP.rapamycin.FRB ternary complex. *J. Am. Chem. Soc. 127*, 4715−4721.

(41) Magliery, T. J., Wilson, C. G., Pan, W., Mishler, D., Ghosh, I., Hamilton, A. D., and Regan, L. (2005) Detecting protein−protein interactions with a green fluorescent protein fragment reassembly trap: Scope and mechanism. *J. Am. Chem. Soc. 127*, 146−157.

(42) Jackrel, M. E., Cortajarena, A. L., Liu, T. Y., and Regan, L. (2010) Screening libraries to identify proteins with desired binding activities using a split-GFP reassembly assay. *ACS Chem. Biol. 5*, 553−562.

(43) Paulmurugan, R., and Gambhir, S. S. (2003) Monitoring protein−protein interactions using split synthetic renilla luciferase protein-fragment-assisted complementation. *Anal. Chem. 75*, 1584−1589.

(44) Wehrman, T., Kleaveland, B., Her, J. H., Balint, R. F., and Blau, H. M. (2002) Protein−protein interactions monitored in mammalian cells via complementation of beta-lactamase enzyme fragments. *Proc. Natl. Acad. Sci. U.S.A. 99*, 3469−3474.

(45) Galarneau, A., Primeau, M., Trudeau, L. E., and Michnick, S. W. (2002) Beta-lactamase protein fragment complementation assays as *in vivo* and *in vitro* sensors of protein−protein interactions. *Nat. Biotechnol. 20*, 619−622.

(46) Nistala, G. J., Wu, K., Rao, C. V., and Bhalerao, K. D. (2010) A modular positive feedback-based gene amplifier. *J. Biol. Eng. 4*, 4.

(47) Lohmueller, J. J., Armel, T. Z., and Silver, P. A. (2012) A tunable zinc finger-based framework for Boolean logic computation in mammalian cells. *Nucleic Acids Res. 40*, 5180−5187.

(48) Lai, K., Kaspar, B. K., Gage, F. H., and Schaffer, D. V. (2003) Sonic hedgehog regulates adult neural progenitor proliferation in vitro and in vivo. *Nat. Neurosci. 6*, 21−27.

(49) Leonard, J. N., Ferstl, P., Delgado, A., and Schaffer, D. V. (2007) Enhanced preparation of adeno-associated viral vectors by using high hydrostatic pressure to selectively inactivate helper adenovirus. *Biotechnol. Bioeng. 97*, 1170−1179.

(50) Kafri, T., van Praag, H., Gage, F. H., and Verma, I. M. (2000) Lentiviral vectors: Regulated gene expression. *Mol. Ther. 1*, 516−521.

(51) Landau, N. R., Warton, M., and Littman, D. R. (1988) The envelope glycoprotein of the human immunodeficiency virus binds to the immunoglobulin-like domain of CD4. *Nature 334*, 159−162.

(52) Atasoy, D., Aponte, Y., Su, H. H., and Sternson, S. M. (2008) A FLEX switch targets Channelrhodopsin-2 to multiple cell types for imaging and long-range circuit mapping. *J. Neurosci. 28*, 7025−7030.

(53) Ai, H. W., Shaner, N. C., Cheng, Z., Tsien, R. Y., and Campbell, R. E. (2007) Exploration of new chromophore structures leads to the identification of improved blue fluorescent proteins. *Biochemistry 46*, 5904−5910.

(54) Inoue, T., Heo, W. D., Grimley, J. S., Wandless, T. J., and Meyer, T. (2005) An inducible translocation strategy to rapidly activate and inhibit small GTPase signaling pathways. *Nat. Methods 2*, 415−418.

902

dx.doi.org/10.1021/sb400128g | *ACS Synth. Biol.* 2014, 3, 892−902